# A Cross-Stacked Radiating Antenna With Enhanced Scanning Performance for Digital Beam-Forming Multifunction Phased-Array Radars

José D. Díaz, *Student Member, IEEE,* Jorge L. Salazar-Cerreno, *Senior Member, IEEE,*
Javier A. Ortíz, *Student Member, IEEE,* Nafati Aboserwal, *Member, IEEE,*
Rodrigo Lebrón, *Student Member, IEEE,* Caleb Fulton, *Senior Member, IEEE,* Robert Palmer, *Fellow, IEEE*

***Abstract*—This contribution presents the results of a dual polarized radiating element designed to achieve low cross polarization (lower than -40 dB measured for the E- and H-plane, at least -30 dB in the D-plane based on simulations) and large fractional bandwidth (18%) over wide scanning angles ($\pm$ 60°). The proposed design includes multiple features that enable high isolation between ports, reduction of spurious radiation, highly symmetrical radiated fields, and suppression of diffracted fields between contiguous sub-array gaps. To verify the polarimetric requirements for weather radar, simulated and measured results, including electronic scanning of the array and embedded element patterns of the antenna are shown.**

***Index Terms*—microstrip patch antenna, cross-patch antenna, stacked patch, wideband, wide angle, dual-polarized, aperture-coupled, phased-array radar, digital beamforming, multifunction phased array radar (MPAR).**

## I. Introduction

The multifunction phased array radar (MPAR) initiative presented an opportunity for the design of high-performance antenna elements that are capable of atmospheric interrogation and aircraft surveillance. Some antenna architectures have been proposed to comply with the dual-polarization demand [1]–[7], but little has been reported compiling weather requirements and design considerations for MPAR antennas. Depending on the architecture of the array, the performance of these elements will be exposed to different scenarios that drive the performance of the whole array. Series feed antenna architectures [1], [2] allow for a reduced number of Tx and Rx channels, while the complexity in the design of the antenna is increased. The same is true for overlapped subarrays [3], for which beamforming architectures present another challenge independent from the design of the antenna element. These techniques are examples of experimental MPAR beamforming concepts that are continuing to be tested today to satisfy the weather and aircraft surveillance needs of this mission.

As a part of this initiative, the Advanced Radar Research Center (ARRC) proposed a fully digital, element level digitization MPAR line replaceable unit [4] that allows for highly flexible fast scanning strategies and beamforming techniques [8]. Element level control, in this context, is the ability to operate a dual-polarized antenna element with individual channels for both H- and V-polarization. The design of such array frontends is considerably easier than any other antenna architecture, while significantly more challenging for the array back-end. From an antenna designer's perspective, the performance of a big array with this level of control will be determined by the embedded antenna element characteristics. For example, the cross-polarization level in an array where all elements are identical is defined by the embedded element pattern and the array factor [9]. Moreover, the embedded element pattern is also related to the active impedance of the array [10], which defines the efficiency of the antenna as it scans. These features are important to understand since they describe the performance of the array in terms of the antenna element from which it is designed.

Now that the importance of the antenna element is established, the MPAR requirements will dictate the selection of the antenna. Bandwidth, isolation, cross-polarization, scanning performance, and manufacture tolerances are some of the most crucial factors that must be considered in the selection of the element. Co-polar patterns with differences of 0.1 dB between polarizations and cross-polarization levels lower than -40 dB are required within a scanning range of $\pm$ 45°. These requirements are to date some of the most constraining for dual-polarized phased array radars [11], [12].

Numerous techniques to design and improve the performance of microstrip patch antenna elements have been discussed [9], [13]–[15]. These articles comprehensively cover different aspects of the design of microstrip patch antennas and provide guidelines for their use in phased arrays. It is in the interest of this work to review some of the methods discussed in previous contributions while narrowing the techniques that can be applied to comply with antenna weather requirements for the MPAR initiative. A dual, linearly polarized aperture-coupled, cross-stacked microstrip patch radiating element is presented and proves to overcome scanning losses while showing low cross-polarization through the whole scanning range of interest.

In section II, a discussion of current trends in the design tradeoffs of high-performance radiating elements is developed with enfaces to overcome bandwidth, cross-polarization, and manufacturability issues. Section III discusses all applied techniques to design the antenna element and its array including simulated results. Section IV of this contribution presents the

J. Diaz, J. Salazar, J. Ortiz, and N. Aboserwal, R. Lebron, C. Fulton, and R. Palmer are with the Advanced Radar Research Center and the Department of Electrical and Computer Engineering, The University of Oklahoma, Norman, OK, 73019 USA, see http://www.arrc.ou.edu.

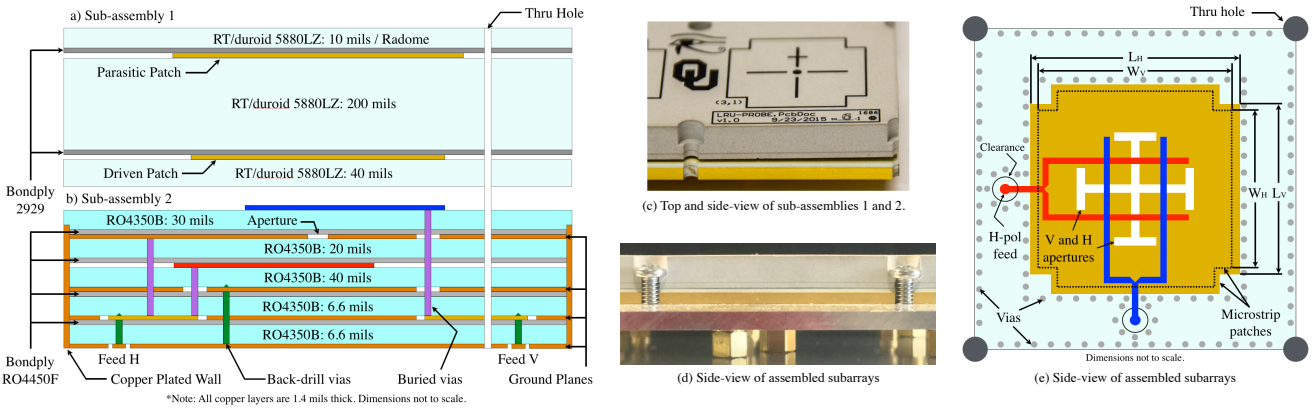


Fig. 1: (a) Stack-up of the radiator assembly for the subarrays with the materials and heights used for the design. (b) Stack-up of the feeding network assembly for the subarrays with the materials and heights used for the design. (c) Top and side view of the manufactured subarrays. (d) Side-view of the assembled manufactured subarrays. (e) Top-view of the antenna element.

performance of the embedded antenna element and the measured scanning capabilities of the array in far-field and near-field ranges. In Section V, the most important contributions and achievements in the antenna community resulting from this work for the MPAR mission are detailed.

## II. Antenna Design Tradeoffs

The goals for the performance of the antenna element were first presented in [4]. In that contribution, the simulated results for the antenna element on a $\lambda_o/2$ ground plane included active reflection coefficients, cross-polarization levels in the principal planes, and preliminary antenna pattern measurements at the array level. In Sections A through C, the authors discuss which factors were involved in the selection of the antenna architecture that provided these results.

### A. Bandwidth

One of the main drawbacks of using microstrip patch antennas is their limited impedance bandwidth [13]- [15]. This limitation is even more evident in phased array antennas when sometimes a need for different feeding networks for specific elements can result in a reduction of the impedance bandwidth of the array. Using a thick material with a low dielectric constant could potentially overcome the bandwidth difficulty. However, surface waves can propagate as the thickness of the dielectric is increased [15]. In a case where a bandwidth of 10% is expected for a material with a dielectric constant of 2.2, the resultant thickness is approximately $0.07\lambda_o$ for a single patch, according to [16]. This is a clear constraint for practical microstrip patch antenna arrays that are designed for low frequencies, given that these thicknesses typically exceed manufacturing industry standards. One way to avoid the use of thick materials, which improves the bandwidth, is using multisection matching networks with the antenna element. However, size constraints of the unit cell (typically $0.5\lambda_o$) make multisection matching networks difficult to apply in planar arrays [16]. Another approach to improve the bandwidth is to use the stacked patch configuration, which offers an increased aperture efficiency of the antenna when compared to a single patch element [17]. This technique allows for a reduction in the dielectric thickness required to achieve the same bandwidth when compared to a single patch antenna. Section III of this work presents the design approach that combined several techniques including the cross-stacked patch as shown in Fig. 1. This approach enabled 18% impedance bandwidth for the presented antenna element.

### B. Isolation & Cross-Polarization

The isolation and cross-polarization levels of dual-polarized microstrip patch antennas are determined by unwanted excited modes, which are related to the physical characteristics of the radiator such as dielectric thickness, width, length, and feeding network of the patch [18], [19]. In terms of today's radar design requirements, cross-polarization levels for simultaneous and alternate transmission are on the order of -40 and -20 dB, corresponding to an accuracy in differential reflectivity below 0.2 dB [11]. Techniques for arrays and elements have been discussed in the literature to suppress cross-polarized radiation. At the array level, mirroring of antennas lowers the overall cross-polarization of the array due to the cancelation of fields coming from neighboring elements [20].

At the element, balanced probe-fed microstrip patches have reached cross-polarization levels of -30 dB with a significant increase in complexity due to the hybrid feeding network needed to produce the proper phase between the excitations [5]. Moreover, this technique requires the connection of 2 or 4 probes directly soldered to the microstrip patch, and in an array with thousands of elements, the large number of solder joints could reduce the reliability of the system [15]. Another approach to suppress cross-polarization on the antenna element is defective ground structures (DGS) [21], [22]. DGS had proven to reduce cross-polarization levels in microstrip patch antennas to the same level of the balanced feed configuration. It is important to notice that DGS are often used for probe-fed or in-set fed linearly polarized microstrip patch antennas.

Considering non-contacting feeds, aperture-coupled microstrip antennas generally offer a more robust design because their construction lacks soldered feed pins [23]. An aperture

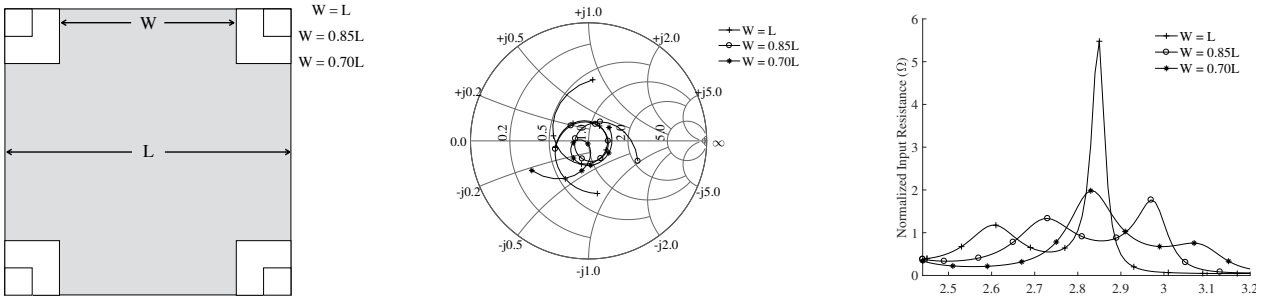


Fig. 2: (a) Top view of the cross-patch antenna element with variations on the width: W = L, W = 0.85L, and W = 0.70L. (b) Normalized ($50\Omega$) real part of the input impedance across frequencies in the cross-patch antenna element as the ratio of *W/L* decreases. (c) Loci of the normalized input impedance as the ratio of *W/L* decreases.

is located on a ground plane that separates both vertical and horizontal polarization. Each feeding network couples to the aperture, while the aperture then couples the energy to the driven patch. A cross-sectional view of this mechanism using stacked patches is shown in Fig. 1(a) and 1(b). This technique allows for high isolation between ports which is inherently related to the cross-polarization level [24]. On the downside, the construction of this configuration is difficult and the back-lobe radiation is higher than the traditional probe-fed patch due to the energy coming from the slot [25]. In order to reduce the radiation that comes from the slot, a feeding network based on striplines with a backing ground plane could be used for one of the polarizations as shown in Fig. 1(a) and 1(b). In terms of cross-polarization, this technique shows better performance than other feeding methods when the apertures are designed to keep cross-polarized radiation away from broadside [26]. In Section III, it is shown that isolation levels below -48 dB are possible in the element while the scanned cross-polarization can be maintained below -40 dB.

### C. Manufacturability

The performance against the temperature of the antenna should be as constant as possible to avoid uncertainty in the calibration of the array. Besides having a low dielectric constant, the materials on a stacked patch configuration should have similar thermal expansion coefficients (TEC) to prevent misalignment of the radiators during manufacturing or operation of the array (see Table I). Using different materials for multilayer structures (i.e., with different TECs) is not encouraged due to various rates of expansion that could occur across surfaces. Most active phased array antennas for radar applications, especially the long-range radars, requires transmitting peak power in the order of several kilowatts. Power dissipation in the antenna front-end can easily delaminate or warp the multilayer structure degrading the overall performance of the array. In some cases, warping of the multilayer antenna array can occur during the manufacturing process. To avoid this warping is recommended the use of balance multilayer structures. Unfortunately, using balance stack-up is not always good for high RF performance. To minimize this issue, the proposed antenna array was constructed by

TABLE I: Antenna materials used for the design

| Materials | TEC: X, Y, Z | $\epsilon_r$ | Dissipation Factor |
|---|---|---|---|
| RO4350B | 10, 12, 32 | 3.66 | 0.0031 |
| RO4450F | 19, 17, 50 | 3.52 | 0.0040 |
| 2929 Bondply | 50, 50, 50 | 2.94 | 0.0030 |
| RT/duroid 5880LZ | 44, 43, 41.5 | 1.96 | 0.0019 |

stacking two independent assemblies, as shown in Fig. 1(a) and 1(b). With this approach, lamination cycles for each sub-assembly are reduced independently when compared to a single assembly. To reach the interconnection of the assemblies and the flatness of the mounted array, screws around the elements are placed and tighten as seen in Fig. 1(c) and 1(d).

## III. Design Approach

### A. Antenna and Feeding Network

After reviewing different types of feeding networks, a non-contact feed network was chosen. A non-contact feed network allows for high isolation between polarizations, thus channel interactions are suppressed. The feeding network discussed in [27] allows for both polarizations to coexist while being separated by a ground plane. The results of this separation is exceptional isolation between polarizations in the order of -40 dB. Moreover, this feeding network allows for having symmetrical apertures on the ground plane. Symmetry is important at the element level in order to cancel near-field interactions that might increase the cross-polarization at the array level and, to maintain similar performance for both H- and V-polarization.

To overcome the bandwidth difficulty, a stacked patch configuration was adopted. The combination of the previously mentioned feeding network with the stacked patch is presented in [28]. To optimize the model, guidelines discussed in [29] were followed, because they apply to dual-polarized antennas. In this design, the excitation of the aperture as a resonant source to increase bandwidth was not employed. In other words, the bandwidth enhancement was only due to the coupling between the cross-stacked microstrip patches. This

consideration is essential, given that the radiation coming from the aperture is not contributing to the radiated fields in the desired bandwidth, which have the potential to jeopardize cross-polarization levels.

For manufacturing purposes, the radiators and the feeding network were separated into two different assemblies to prevent them from de-lamination and bending. The radiator assembly consists of two conducting layers and a radome of RT/duroid 5880LZ bonded with Bondply 2929. The low permittivity values of the dielectrics in the radiator's assembly ensure higher bandwidths. The presence of the radome has little to no effect on the radiated fields and allows for marking the layer with a cross pattern that identifies the center of the antenna element as seen in Fig. 1 (c). This center is going to be recognized by a high-definition camera for calibration purposes [30].

The feeding network assembly is made out of six conducting layers bonded with RO4450F. A more detailed description of the materials used for the array is shown in Table I. The stack up for the array is shown in Figs. 1 (a) and 1 (b). Notice the feeding network assembly uses RO4450F because it has similar electrical properties to RO4350B. Figs 1 (c) and 1 (d) show the side view of manufactured assemblies. It can be seen that when both assemblies are connected, the bend that is present in the radiators and feeding network assemblies disappears because of the screws. Blind plated vias were placed around the periphery of the element below the aperture ground, as shown in Fig. 1 (e), to minimize the interaction between the apertures and feeding networks. To further decrease the presence of any spurious modes, blind plated vias were also put around the H- and V-feeds. To maximize conductivity and isolate the effects of neighboring subarrays, a 10 mil copper-plated wall was included in the feeding network assembly, as shown in Fig. 1 (b-d), which matches the same height of the blind vias.

Until this point, the focus of the discussion has been in the design of the feeding network and the materials employed in the antenna stack-up, yet, the geometry of the radiator also influences the cross-polarization and bandwidth. In general, rectangular microstrip patches exhibit higher bandwidths when the width is greater than the length [16]; however, this geometry does not allow dual-polarization to occur in the microstrip patch. To produce dual-polarization mode operation, a square patch antenna is commonly used. One important limitation of square patch antennas is its high impedance sensitivity and its cross-polarization due to the excitation of higher order modes as a function of the feed position [18], [19], [31]. In this design, the cross-patch ratio (*W/L*) was used to achieve the desired coupling in the antenna element. The features of this treatment are shown in Fig. 2 (a-c). As *W/L* decreases with *L* constant, the impedance loci rotate clockwise (see Fig. 2 (b)), indicating an increase of inductance due to the narrowing of the patch. Concurrently, the operational frequencies of the patches shift higher, as shown in Fig. 2 (c). This result is expected, given that the radiator becomes electrically smaller when compared to a full square patch. Using the cross-patch geometry, the cross-polarization in the antenna is enhanced and there is little effect on the bandwidth when compared to the square geometry. The S-parameters of the proposed antenna element are presented in Fig. 3. The overlapped bandwidth between the polarizations is roughly 400 MHz or 18% (lower than -10 dB), and the isolation between the ports peaks at 2.97 GHz with a value of -48 dB when implementing the cross-stacked patch antenna and the aperture coupling technique.

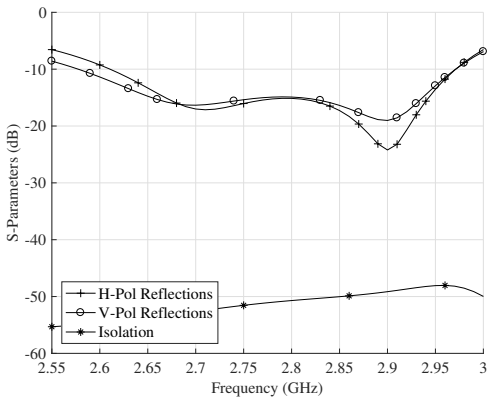


Fig. 3: The simulated isolated antenna element reflections and isolation between polarizations using HFSS.

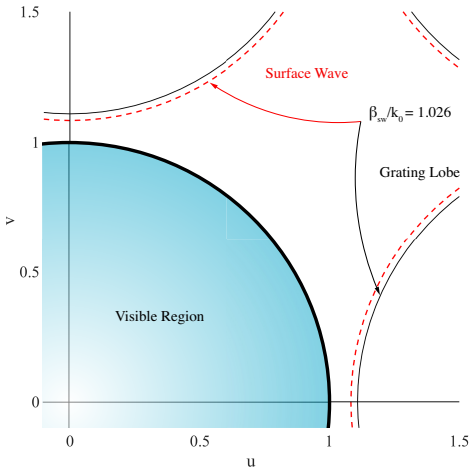


Fig. 4: Grating lobe diagram using a spacing of $d_x = d_y =$ 50.8 mm, an averaged permittivity of 2.14 that includes all dielectrics above the apertured ground plane from Fig. 1 (a), and an operational frequency of 2.8 GHz.

### *B. Antenna Array*

In general, there are two factors involved in scanning performance, the size of the unit cell to minimize the possibility of grating lobes, and surface waves that could allow scan blindness. To avoid the presence of grating lobes in a phased array antenna, the spacing between elements is selected to be lower than $\lambda_o/2$. With a center frequency of 2.8 GHz, the size of a unit cell for a square lattice array is 53.55 mm that corresponds to $\lambda_o/2$, however, the designed array has a spacing of 50.8 mm. A set of simultaneous transcendental equations [32] were used to estimate the boundaries established by the grating lobe diagram given the corresponding spacing of the designed array

TABLE II: Scanning Performance

| | Frequency (GHz) | | |
|---|---|---|---|
| Parameter | 2.7 | 2.8 | 2.9 |
| Element spacing ($d_x$, $d_y$) | 0.457 $\lambda_o$ | 0.474 $\lambda_o$ | 0.491 $\lambda_o$ |
| Surf. waves propag. const. ($\beta_{sw}/k_0$) | 1.0254 | 1.0256 | 1.0285 |
| Scanning range (E-,H and D-planes) | $\pm 45°$ | $\pm 45°$ | $\pm 45°$ |
| Scan blindness in the visible region | none | none | none |

and the radiators assembly properties. An average weighted permittivity that includes all layers in the radiator's assembly and the dielectric of the V-pol transmission line (i.e., the dielectric above the aperture) was calculated to be 2.14, with an overall height of 280 mils or 0.0664 $\lambda_o$.

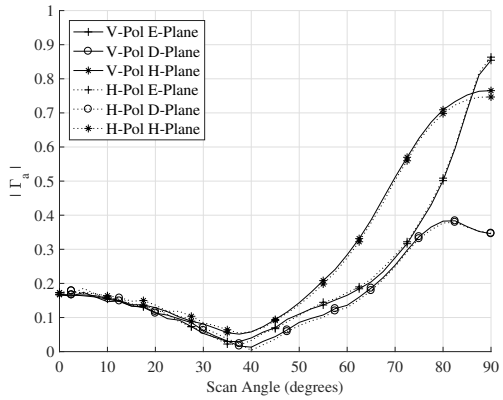


Fig. 5: The simulated active reflection coefficient for the antenna using HFSS at 2.8 GHz.

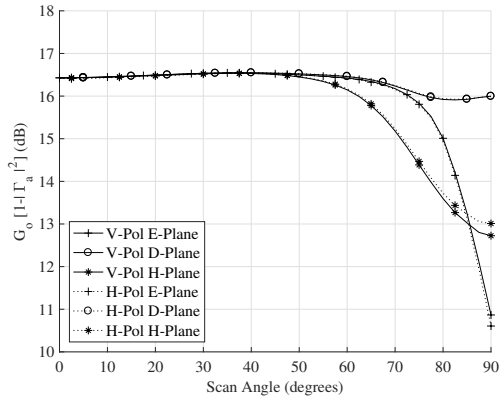


Fig. 6: The simulated gain loss for a 2x8 antenna array using the active reflection coefficient results from Fig. 5.

Fig. 4 shows the grating lobe diagram that illustrates the impact of the surface waves in the visible region at the center frequency. It can be seen that the surface wave contribution added to the diagram yields no gratings lobes in the visible region. The analysis was extended to other frequencies of interest in the antenna and the results are shown in Table II. It can be seen that for the highest operational frequency, the unit cell size is less than $\lambda_o/2$. Higher order modes of surface waves are not excited in the proposed antenna array while parallel plate modes were mitigated using vias in the

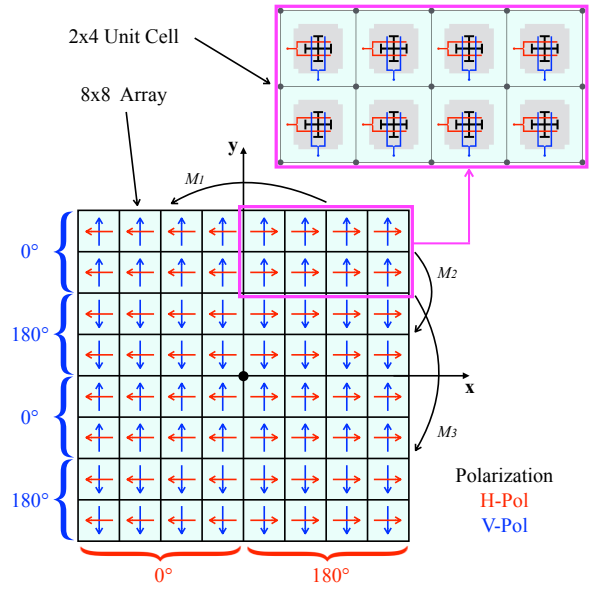


Fig. 7: Resultant polarization of the elements on the 8x8 array when duplicating the 2x4 unit cell using mirror operations. $M_1$, $M_2$, and $M_3$ refer to the applied mirror operations on the 2x4 unit cell parallel to x-, y-, and y-axis, respectively.

transmission line sub-assembly (see Fig. 1(b)). Infinite array numerical simulations of the antenna unit cell in HFSS were used to validate the overall scanning performance of the array. Fig. 5 shows the active reflection coefficient for the antenna element for E-, D-, and H-planes and both polarizations at 2.8 GHz. No scan blindness was found in the principal planes for both polarizations. Fig. 6 shows the gain loss of the antenna using the active reflection coefficient data from the results presented in Fig. 5. It can be seen that less than 0.4 dB loss is expected when the antenna scans to 60°.

To minimize the effects of cross-polarization contamination due to the exposed feeding network (V-polarization), a mirroring technique at the array level was adopted [20]. The method enables the cancellation of near-field interactions between the feed networks exposed above the aperture ground plane. Once designed, the antenna element was expanded into a 2x4 unit cell and the 8x8 array was achieved using the mirror operations shown in Fig. 7. It can be seen that the V-polarization is physically 180° out of phase every 2 rows in the 8x8 array while the H-polarization is mirrored along the y-axis.

## IV. Results

In order to simplify the measurements of the radiation patterns of the array and the antenna element, the authors used polarization based on Ludwig's third definition. However, to accurately describe the cross-polarization away from the principal planes, Ludwig's second definition should be used since microstrip patch antennas are not Huygen sources [33]. In this section, we discuss the measured results of antenna patterns (embedded element and array patterns) performed in a far-field and near-field anechoic chambers at the Radar Innovation Laboratory at the University of Oklahoma.

Measurements for the patterns were first conducted in a far-field range using a customized NSI-RF-WR284 waveguide probe that operates in a frequency range from 2.6 - 3.95 GHz. A customized fixture (see Fig. 8 (a)) constructed of high-performance Rohacell 110 IG/A with $\epsilon_r$ = 1.12 was used to support the array on a pedestal. This feature minimized reflections and disruption of patterns on the specular region of the far-field chamber. The antennas were attached to a solid aluminum plate that extended 1 inch $\left(\frac{1}{2}\lambda_o\right)$ from the border of the array, and the patterns were obtained at 3.0 GHz. As an effort to differentiate between the cross-polarization of the antenna element and the 8x8 array, measurements of the center element on a 3x3 array were performed and results are shown in Fig. 8 (b). It can be seen that highly symmetrical co-polarizations were achieved for both H- and V-polarizations, and in terms of cross-pol, less than -34 dB for the E-planes, better than -32 dB for the H-planes, and about -13 dB for the D-planes were measured.

For the array patterns, measurements for both polarizations were taken while exciting the two middle rows on the 8x8 array. To create the 2x8 array pattern, two 8x1 power combiners are used and connected with coaxial cables. Also, phase shifters were added in elements that were physical off-set 180° due to the antenna mirroring. Fig. 8 (c) shows the measured co- and cross-polarization patterns using Ludwig's 3rd definition. It can be seen that at broadside, the cross-polarization level is below -45 dB for both polarizations in the measured planes from $\pm$ 45° in azimuth. Even though the cross-polarization is close to the values obtained in simulations, the null of the antenna pattern are not well defined. This can be attributed to phase errors induced by the power combiners, cables, and the short distance (20% shorter than the actual far-field estimation) between the antenna array and probe that does not satisfy the minimum distance required for far-field measurement.

In order to obtain the scanning performance of the antenna array and validate the measurements of the far-field range, a 16-channel board that contains digital phase shifter and attenuators was designed and fabricated. Figure 9 (a) shows the active array antenna setup at the OU near-field range, the T/R module board, the control board, and the measured scanned performance of the antenna array using the 2x8 and 8x2 configurations for H- and V-polarization. Measurements were obtained every 5° in a scanning range of $\pm$ 45° for both polarizations in azimuth and elevation planes. To control the phase of the antennas, 6-bit serial control phase shifter and attenuator cards were made with a resolution of 5.625° and 0.5 dB for each element. A calibration algorithm was performed to remove amplitude and phase inaccuracies between channels. Fig. 9 (g-h) shows the co- and cross-polarization of 2 rows (g and i) and 2 columns (h and j) of the scanned array every 5°. It can be seen that the cross-polarization for all cases is roughly below -40 dB for both polarizations in the principal planes. At the time of publication, the resources for scanning the array in the D-plane were not available. For this reason, the scanned cross-polarization of the array was based on a HFSS Domain Decomposition Method (DDM) simulation that did not include the rotation of the elements in the array. The results of this simulation predict cross-polarization below -30 dB for both polarizations when scanning to $\theta_0 = 45°$ and $\phi_0 = 45°$.

## V. Conclusion

The use of multiple techniques for improving the performance of an antenna element that could satisfy today's requirements for phased array weather radars was presented. A new coupling mechanism, the cross-patch ratio, was presented and results show how this parameter could help to achieve the required coupling on an aperture coupled patch antenna. Measured scanning results in a far-field range for 2 rows and 8 columns on an 8x8 array were presented at broadside, and results show cross-polarization levels below -45 dB. To corroborate the far-field measurements, near-field measurements were performed and the results show the same cross-polarization at broadside while a scanning cross-polarization of -40 dB in the principal planes. As the number of elements increase, the authors expect that inaccuracies or phase differences in the cross-polarized radiation coming from the elements will lower further the scanning cross-polarization. In summary, the authors have presented an optimized antenna element for MPAR purposes capable of achieving the bandwidth, isolation, scanning, and cross-polarization requirements for the MPAR mission.

## Acknowledgment

This work was partially supported by NOAA's National Severe Storms Laboratory under CIMMS cooperative agreement NA11OAR4320072. The authors would like to thank Jon Christian and Redmond Kelley for their contributions in constructing the fixture used to measure the antennas. In addition, we wish to express our appreciation to Redmond Kelley for assisting in the development of the manufacturing files of the subarrays. Special thanks are in order to: Alessio Mancini, Simon Duthoit, Brian Brown, Kevin Constien, David Hayes and Thomas Brachtenbach for their help in the measurements.

## References

[1] J. L. Salazar, E. J. Knapp, and D. J. McLaughlin, "Dual-Polarization Performance of the Phase-Tilt Antenna Array in a CASA Dense Network Radar," *2010 IEEE International Geoscience and Remote Sensing Symposium*, pp. 3470–3473, 2010.

[2] S. Karimkashi and G. Zhang, "A Dual-Polarized Series-Fed Microstrip Antenna Array With Very High Polarization Purity for Weather Measurements," *IEEE Transactions on Antennas and Propagation*, vol. 61, no. 10, pp. 5315–5319, 2013.

[3] J. Herd and S. Duffy, "Overlapped Digital Subarray Architecture for Multiple Beam Phased Array Radar," *Antennas and Propagation (EUCAP), Proceedings of the 5th European Conference on*, pp. 3027–3030, 2011.

[4] J. Diaz, J. Salazar, J. Ortiz, C. Fulton, N. Aboserwal, R. Kelley, and R. Palmer, "A Dual-Polarized Stacked Patch Antenna with Wide-Angle and Low Cross-Polarization for Fully Digital Multifunction Phased Array Radars," in *Fifth International Symposium on Phased Array Systems and Technology*, Boston, MA, 2016.

[5] C. Fulton and W. Chappell, "A Dual-Polarized Patch Antenna for Weather Radar Applications," in *2011 IEEE International Conference on Microwaves, Communications, Antennas and Electronic Systems (COMCAS 2011)*, vol. 2, no. 2. IEEE, nov 2011, pp. 1–5.

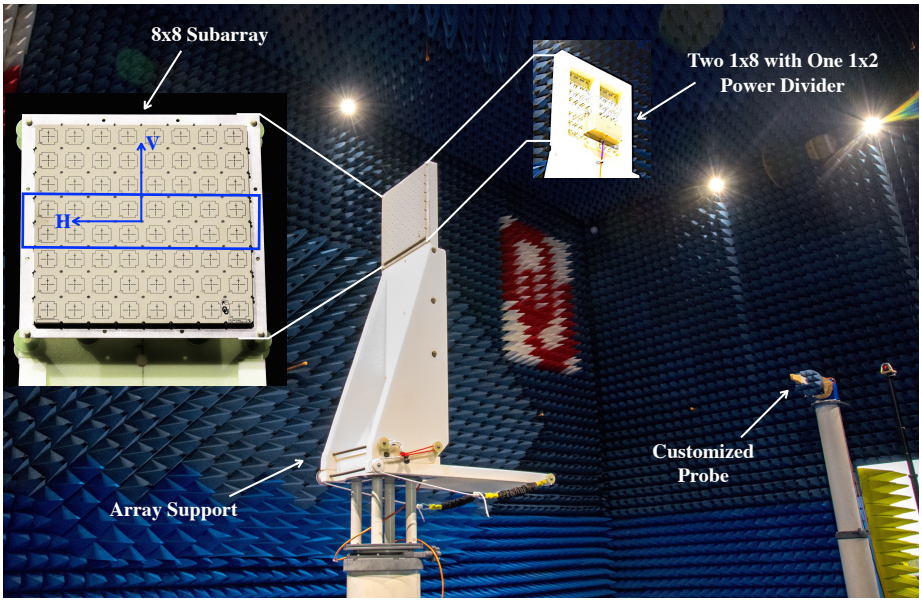


(a) Far-field measurement setup for the antenna arrays

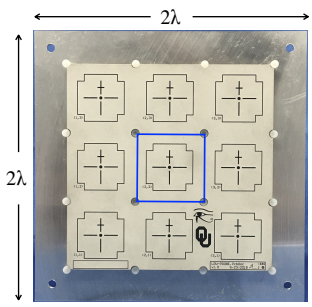


(b) 3x3 Subarray

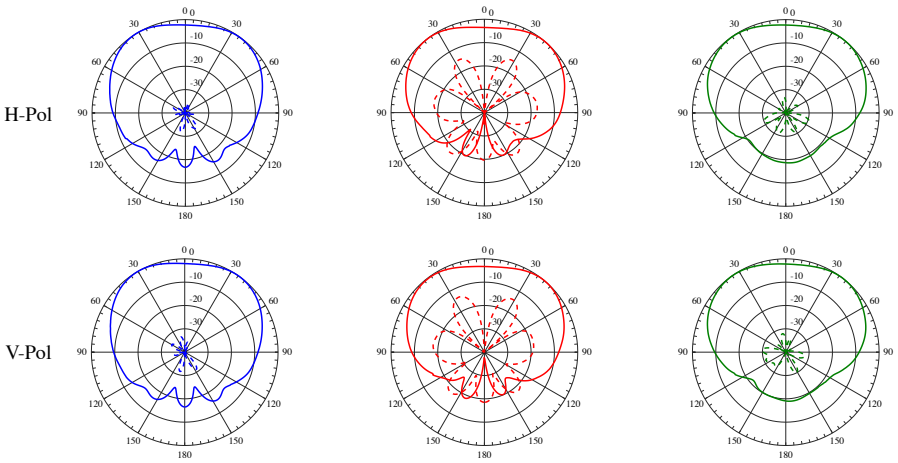


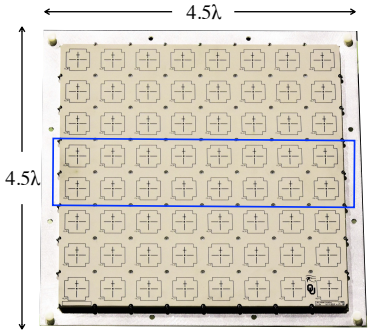


(c) 8x8 Subarray

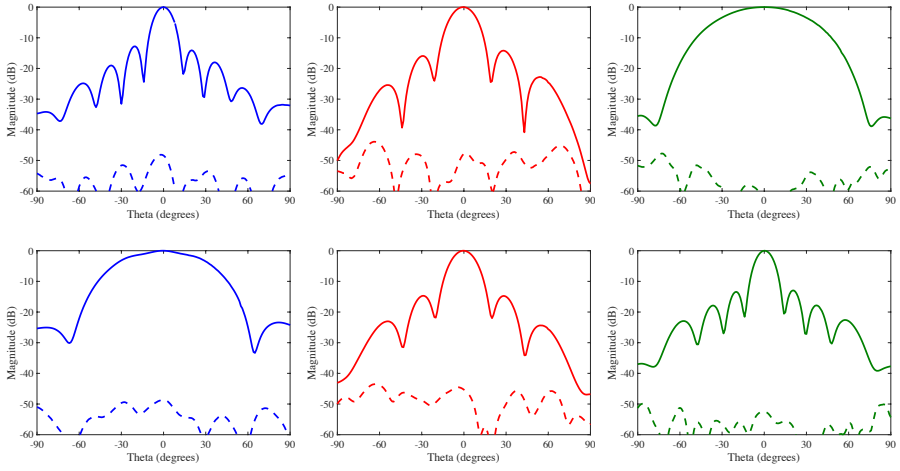


E-Plane D-Plane H-Plane

Fig. 8: (a) Far-field chamber used for the setup and measurements of the antenna subarrays. (b) Measured radiation patterns at 3.0 GHz for H- and V-polarizations on the center element of the 3x3 subarray mounted on a ground plane that protrudes $\lambda_o/2$ from the antenna. (b) Measured radiation patterns at 3.0 GHz for H- and V-polarizations on the 8x8 subarray mounted on a ground plane that protrudes $\lambda_o/2$ from the antenna. Solid (–) and dashed (- -) lines refer to co- and cross-polarization.

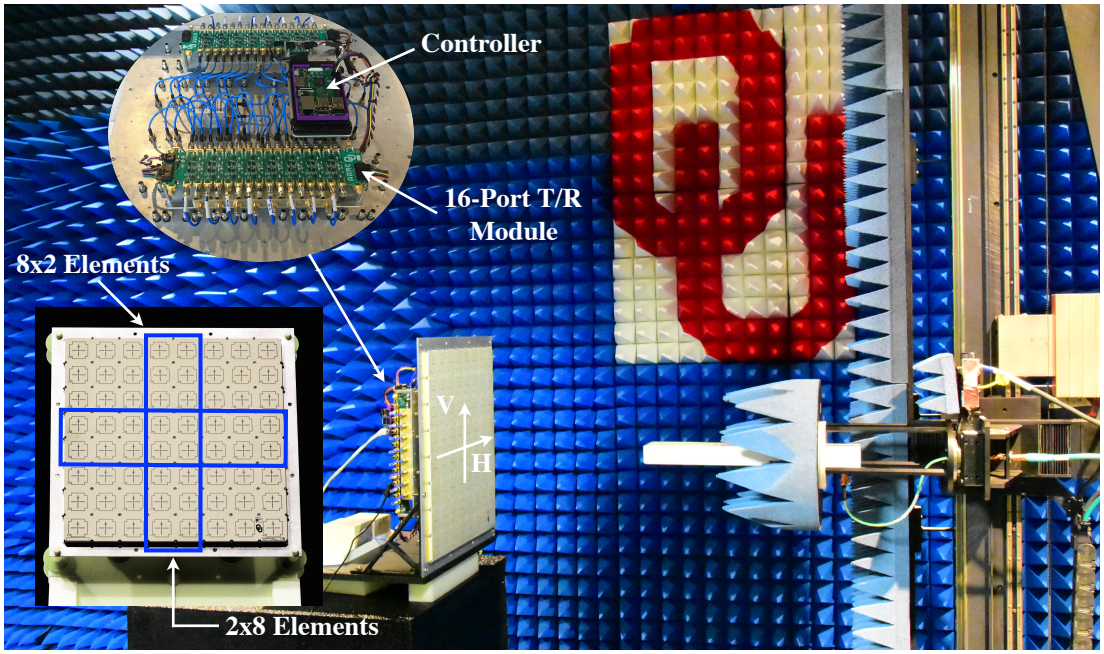


(a) Nearfield measurement setup for the antenna array

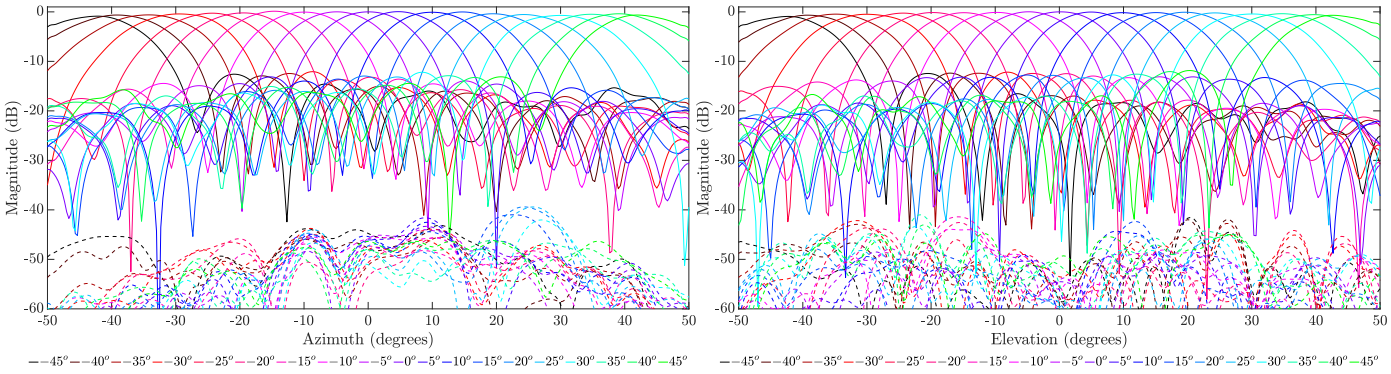


(b) H-Polarization Azimuth Scan (c) H-Polarization Elevation Scan

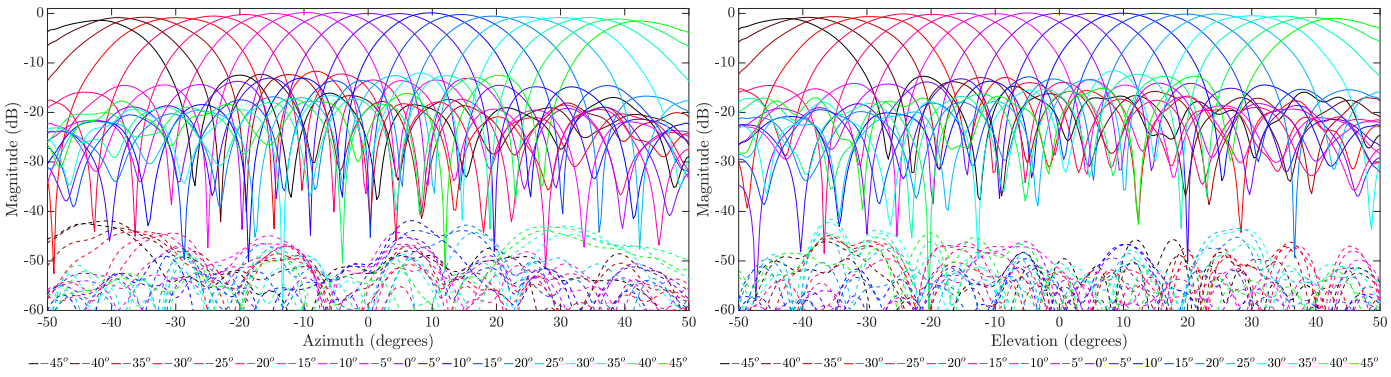


(d) V-Polarization Azimuth Scan (e) V-Polarization Elevation Scan

Fig. 9: Near-field chamber setup for electronically scanned radiation patterns of an array 2x8 elements embedded in an array of 8x8 elements at 3 GHz. (b-d) Measured radiation patterns of 2x8 array (for H- and V-polarizations) in the azimuth plane. (c-e) Measured radiation patterns of 2x8 array (for H- and V-polarizations) in the elevation plane. Solid (–) and dashed (- -) lines refer to co- and cross-polarization.

[6] J. L. Salazar, E. Loew, P.-S. Tsai, J. Vivekanandan, W. C. Lee, and V. Chandrasekar, "Design and Development of a 2-D Electronically Scanned Dual-Polarization Line-Replaceable-Unit (LRU) for Airborne Phased Array Radar for Atmospheric Research," *Preprints Proceedings of 36th International Conference on Radar Meteorology*, vol. 64, no. 1, pp. 1–6, 2013.

[7] J. Salazar, "Dual-polarized radiating patch antenna," U.S. Patent 20160079672 A1, March 17, 2016.

[8] M. C. Leifer, V. Chandrasekar, and E. Perl, "Dual-Polarized Array Approaches for MPAR Air Traffic and Weather Radar Applications," in *2013 IEEE International Symposium on Phased Array Systems and Technology*. IEEE, Oct 2013, pp. 485–489.
[9] D. Pozar and B. Kaufman, "Design Considerations for Low Sidelobe Microstrip Arrays," *IEEE Transactions on Antennas and Propagation*, vol. 38, no. 8, pp. 1176–1185, 1990.
[10] R. Mailloux, *Phased Array Antenna Handbook*. Artech House, 2005.
[11] Y. Wang and V. Chandrasekar, "Polarization Isolation Requirements for Linear Dual-Polarization Weather Radar in Simultaneous Transmission Mode of Operation," *IEEE Transactions on Geoscience and Remote Sensing*, vol. 44, pp. 2019–2028, 2006.
[12] D. S. Zrnic and R. J. Doviak, "System Requirements for Phased Array Weather Radar," NOAA/NSSL, Tech. Rep., 2005.
[13] K. Carver and J. Mink, "Microstrip Antenna Technology," *IEEE Transactions on Antennas and Propagation*, vol. 29, no. 1, pp. 2–24, 1981.
[14] K. C. Gupta, "Broadbanding Techniques for Microstrip Patch Antennas - A Review," University of Colorado, Tech. Rep., 1988.
[15] D. Pozar, "Microstrip Antennas," *Proceedings of the IEEE*, vol. 80, no. 1, pp. 79–91, 1992.
[16] D. M. Pozar, "A Review of Bandwidth Enhancement Techniques for Microstrip Antennas," in *Microstrip Antennas: The Analysis and Design of Microstrip Antennas and Arrays*, D. M. Pozar and D. H. Schaubert, Eds. IEEE Press, 1995, ch. 4, pp. 157–166.
[17] A. Sabban, "A New Broadband Stacked Two-Layer Microstrip Antenna," *Antennas and Propagation Society International Symposium, 1983*, vol. 21, pp. 63–66, 1983.
[18] S. Gao, "Microstrip Antenna Elements and Dual-Polarized Arrays for Active Integration," Ph.D. dissertation, Shanghai University, 1999.
[19] S. Gao, L. Li, and P. Gardner, "Recent Research Developments in Microwave Theory & Techniques," in *Dual-polarized antennas for wireless communications and radar systems*, B. Beker and Y. Chen, Eds. Research Signpost, 2002, ch. 8, pp. 1–28.
[20] K. Woelder and J. Granholm, "Cross-Polarization and Sidelobe Suppression in Dual Linear Polarization Antenna Arrays," *IEEE Transactions on Antennas and Propagation*, vol. 45, no. 12, pp. 1727–1740, 1997.
[21] D. Guha, M. Biswas, and Y. Antar, "Microstrip Patch Antenna With Defected Ground Structure for Cross Polarization Suppression," *Antennas and Wireless Propagation Letters*, vol. 4, no. 1, pp. 455–458, 2005.
[22] C. Kumar, M. I. Pasha, and D. Guha, "Microstrip patch with nonproximal symmetric defected ground structure (dgs) for improved cross-polarization properties over principal radiation planes," *IEEE Antennas and Wireless Propagation Letters*, vol. 14, pp. 1412–1414, 2015.
[23] D. M. Pozar and S. M. Duffy, "A Dual-Band Circularly Polarized Aperture-Coupled Stacked Microstrip Antenna for Global Positioning Satellite," *IEEE Transactions on Antennas and Propagation*, vol. 45, no. 11, pp. 1618–1625, 1997.
[24] D. M. Pozar, "Microstrip Antenna Aperture-Coupled to a Microstripline," *Electronics Letters*, vol. 21, no. 2, p. 49, 1985.
[25] K. F. Lee and K. M. Luk, *Microstrip Patch Antennas*. Imperial College Press, 2010.
[26] X. Yang and L. Shafai, "Characteristics of Aperture Coupled Microstrip Antennas with Various Radiating Patches and Coupling Apertures," *IEEE Transactions on Antennas and Propagation*, vol. 43, no. 1, pp. 72–78, 1995.
[27] M. Yamazaki, E. Rahardjo, and M. Haneishi, "Construction of a Slot-Coupled Planar Antenna for Dual Polarization," *Electronics Letters*, vol. 30, no. 22, p. 1814, 1994.
[28] A. A. Serra, P. Nepa, G. Manara, G. Tribellini, and S. Cioci, "A Wide-Band Dual-Polarized Stacked Patch Antenna," *IEEE Antennas and Wireless Propagation Letters*, vol. 6, pp. 141–143, 2007.
[29] F. Croq and D. Pozar, "Millimeter-Wave Design of Wide-band Aperture-coupled Stacked Microstrip Antennas," *IEEE Transactions on Antennas and Propagation*, vol. 39, no. 12, pp. 1770–1776, Dec 1991.
[30] R. Lebron, J. Salazar, C. Fulton, D. Schmidt, and R. Palmer, "A Novel Near-Field Scanner for Millimeter-Wave of Active Phased Array Antenna Calibration for Surface, Thermal, and RF Characterization," in *Fifth International Symposium on Phased Array Systems and Technology*, Boston, MA, 2016.
[31] T. M. F. Elshafiey, "Full Wave Analysis of a Ferrite Cross-Patch Antenna," in *2007 Loughborough Antennas and Propagation Conference*, no. April. IEEE, Apr 2007, pp. 197–200.
[32] D. M. Pozar, *Microwave Engineering*, 4th ed. John Wiley and Sons, 2012.
[33] N. A. Aboserwal, J. L. Salazar, I. Senior, and C. F. Ieee, "Current Polarization Impact on Cross-Polarization Definitions for Practical Antenna Elements," in *Fifth International Symposium on Phased Array Systems and Technology*, 2016, pp. 1–5.

**Jose D. Diaz** (S'12) received the B.S. degree in Electrical and Computer Engineering, and a Curriculum Sequence in Atmospheric Sciences and Meteorology in 2015, from the University of Puerto Rico at Mayagüez (UPRM). He spent 4 years as an undergraduate research assistant for the X-band radar network from the Collaborative Adaptive Sensing of the Atmosphere (CASA) Laboratory. Along with undergraduate studies, he had the opportunity to be an intern for the National Weather Service in Miami, Florida, where research on hail storms in the peninsula was being conducted. In the National Center for Atmospheric Research, Earth Observing Laboratory, research on electromagnetic scattering and wave propagation were his topics for a summer. Diaz became a research assistant in the Advanced Radar Research Center (ARRC) in 2015, under the supervision of Dr. Jorge Salazar at The University of Oklahoma (OU). Today he is pursuing his Ph. D. in Electrical and Computer Engineering with a focus on high-performance antenna elements for phased array radars.

**Dr. Jorge L. Salazar** (S'00-M'12-S'14) received the M.S. degree in electrical engineering from the University of Puerto Rico, Mayagüez, in 2003. He received his Ph.D. from the University of Massachusetts, Amherst, in July 2012. In 2012 Salazar was awarded a prestigious National Center for Atmospheric Research (NCAR) Advanced Study Program Postdoctoral (ASP) Fellowship. In March 2012 he joined the Department of Electrical and Computer Engineering at the University of Puerto Rico, Mayagüez, as an Adjunct Professor. In July 2012 he also joined the Advanced Radar Research Center (ARRC) and the Department of Electrical and Computer Engineering at the University of Oklahoma (OU), Norman, as a Research Scientist and then as an Assistant Professor. His research interests are radar for microwave remote sensing, active phased array radars, antenna design, T/R modules, and electromagnetic scattering and propagation. Dr. Salazar is a member of the Tau Beta Pi honor society of IEEE Geoscience and Remote Sensing, IEEE Transactions in Antennas and Propagation, Aerospace and Electronic Systems.

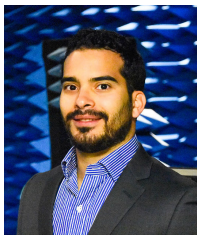

**Javier. A. Ortiz** (S'10) received his B.Sc. degree in electrical engineering from the University of Puerto Rico, Mayagüez, PR, in 2013. He is currently pursuing his Ph.D. degree at the University of Oklahoma, Norman, OK. During his time at the University of Puerto Rico, Ortiz worked as an undergraduate research assistant on projects in electromagnetics. In 2012 he co-founded an IEEE MTT/GRS/APS Joint Chapter and was president from 2012 to 2014. From 2013 to 2014 he worked as a volunteer laboratory teaching assistant and graduate research assistant at the university's Puerto Rico Weather Radar Network. Currently, he is working as a graduate research assistant at the Advanced Radar Research Center at the University of Oklahoma. His research interests involve microstrip patch antennas, modal analysis and filtering, high-purity radiating element designs, and high-performance active phased array antennas.

**Nafati A. Aboserwal** (S'13-M'16) received the B.S. degree in electrical engineering from Al-Mergheb University, Alkhoms, Libya, in 2002. He received his M.S. and Ph.D. degrees in electrical engineering from Arizona State University, Tempe, AZ, in 2012 and 2014, respectively. In January 2015 he joined the Advanced Radar Research Center (ARRC) and the Department of Electrical and Computer Engineering at the University of Oklahoma (OU), Norman, as a Postdoctoral Research Scientist and then as an Anechoic Chamber Manager. His research interests include EM theory, computational electromagnetics, antennas, and diffraction theory. His research also focuses on active high-performance phased array antennas for weather radars, higher modes, and surface waves characteristics of printed antennas, and high performance dual-polarized microstrip antenna elements with low cross-polarization. Dr. Aboserwal is a member of the IEEE Transactions on Antennas and Propagation.

**Rodrigo M. Lebron** (S'16) was born in Asuncion, Paraguay. He received the B.S. degree in Mechatronics from the Universidad Nacional de Asuncin, in 2012, and the M.S. degree in mechanical engineering from the Universidade Federal do Rio Grande do Sul, RS, Brazil, in 2015. He enrolled at the University of Oklahoma on Fall 2015 in the electrical and computer engineering Ph.D. program, where he works as a graduate research assistant in the Advanced Radar Research Center. His research interests include design and development of automated systems for measurement, characterization, and calibration of phased array antennas.

**Dr. Caleb Fulton** (S'05-M'11-S'16) received his B.S. and Ph.D. in ECE from Purdue University in West Lafayette, IN, in 2006 and 2011, respectively, and is now an Assistant Professor in ECE at the University of Oklahoma's Advanced Radar Research Center in Norman, OK. His work focuses on antenna design, digital phased array calibration and compensation for transceiver errors, calibration for high-quality polarimetric radar measurements, integration of low-complexity transceivers and high-power GaN devices, and advanced digital beamforming design considerations. He is currently involved in a number of digital phased array research and development efforts for a variety of applications. He received the Purdue University Eaton Alumni Award for Design Excellence In 2009 for his work on the Army Digital Array Radar (DAR) Project. He also received the Meritorious Paper Award for a summary of these efforts at the 2010 Government Microcircuit Applications and Critical Technologies Conference. More recently, he received a 2015 DARPA Young Faculty Award for his ongoing digital phased array research. Dr. Fulton is a member of the IEEE Antennas and Propagation, Aerospace and Electronic Systems, and Microwave Theory and Techniques Societies, and serves on the Education Committee of the latter.

**Dr. Robert D. Palmer** (S'86-M'89-S'93-F'17) Robert D. Palmer was born in Fort Benning, GA on June 3, 1962. He received the Ph.D. degree in electrical engineering from the University of Oklahoma, Norman, in 1989. From 1989 to 1991, he was a JSPS Postdoctoral Fellow with the Radio Atmospheric Science Center, Kyoto University, Japan, where his major accomplishment was the development of novel interferometric radar techniques for studies of atmospheric turbulent layers. After his stay in Japan, Dr. Palmer was with the Physics and Astronomy Department of Clemson University, South Carolina. From 1993 to 2004, he was a part of the faculty of the Department of Electrical Engineering, University of Nebraska, where his interests broadened into areas including wireless communications, remote sensing, and pedagogy. Soon after moving to the University of Oklahoma (OU) as the Tommy C. Craighead Chair in the School of Meteorology in 2004, Dr. Palmer established the interdisciplinary Advanced Radar Research Center (ARRC). He currently serves as the Executive Director of the ARRC and OU's Associate Vice President for Research. While at OU, his research interests have focused on the application of advanced radar signal processing techniques to observations of severe weather, particularly related to phased-array radars and other innovative system designs. He has published widely in the area of radar remote sensing of the atmosphere, with an emphasis on generalized imaging problems, spatial filter design, and clutter mitigation using advanced array/signal processing techniques. Prof. Palmer is a Fellow of the American Meteorological Society and has been the recipient of several awards for both his teaching and research accomplishments.